Electronic Supplementary Information

Carbon source self-heating: ultrafast, energy-efficient and room temperature synthesis of highly fluorescent N, S-codoped carbon dots for quantitative detection of Fe(III) ions in biological samples

Honggang Yin,‡[a] Die Gao,‡[a] Yan Qiu,[a] Gaoyi Yi,[a] Jun Li,[b] Yingying Dong,[b] Kailian Zhang,*[a] Zhining Xia[c] and Qifeng Fu *[a]

[a.] School of Pharmacy, Southwest Medical University, Luzhou, Sichuan, 646000, China.

[b.] Institute of Engineering Thermophysics, School of Energy and Power Engineering, Chongqing University, Chongqing 400030, China.

[c.] School of Pharmaceutical Sciences, Chongqing University, Chongqing, 401331, China.

* Corresponding Author. E-mail: fuqifeng1990@163.com (Q. Fu); zkl66@swmu.edu.cn (K. Zhang)

‡ These authors contributed equally.

1. Quantum yield measurement

The quantum yield of N, S-codoped CDs was measured by a relative method. Quinine sulfate in 0.1 M H_2SO_4 (quantum yield is 0.54 at 360 nm) was chose as a standard. The quantum yield of a sample was then calculated according to the following equation:

$$\varphi_x = \varphi_{st} \times \frac{\eta_x^2}{\eta_{st}^2} \times \frac{m_x}{m_{st}}$$

where the subscripts "st" and "x" denote the standards and samples respectively, φ is the fluorescence quantum yield, m is the slop determined by the curves of integrated fluorescence intensity vs absorbance, and η is the refractive index with 1.33 as the default for both quinine sulfate and samples. To minimize reabsorption effects, the absorbance values in the 10 mm fluorescence cuvette were kept under 0.1 at the excitation wavelength (360 nm).

2. Additional Results

Fig. S1 The typical photograph of the lyophilized N, S-codoped CDs powder.

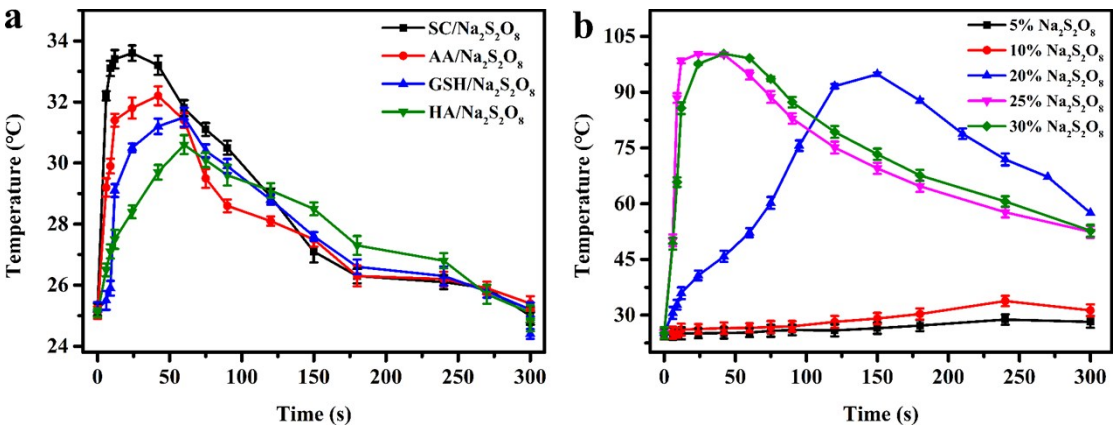

Fig. S2 (a) The temperature change of the mixed solutions composed of the organic reductants (SC, AA, GSH and HA) and $Na_2S_2O_8$ within 5 min; (b) the influence of $Na_2S_2O_8$ concentration on the temperature change of the TEPA/$Na_2S_2O_8$ mixed solutions.

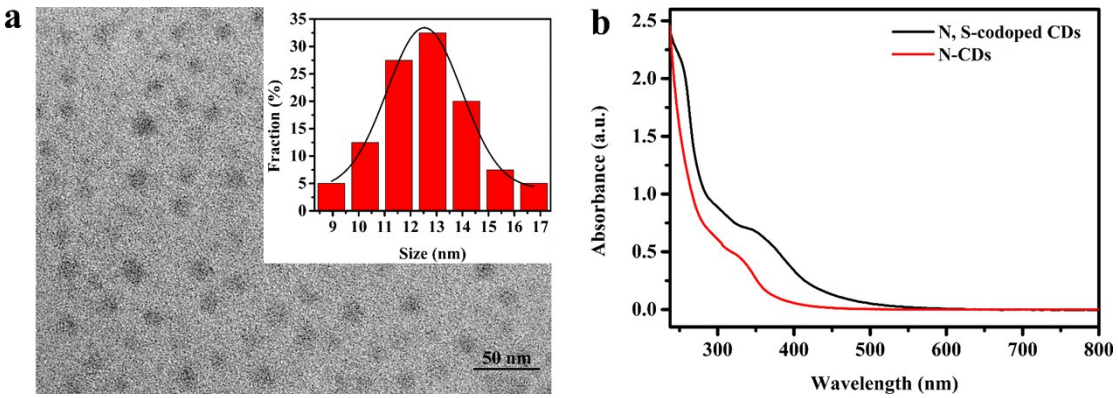

Fig. S3 (a) The typical TEM image of the as-prepared N-CDs; (b) UV-visible absorption spectra of the obtained N, S-codoped CDs and N-CDs.

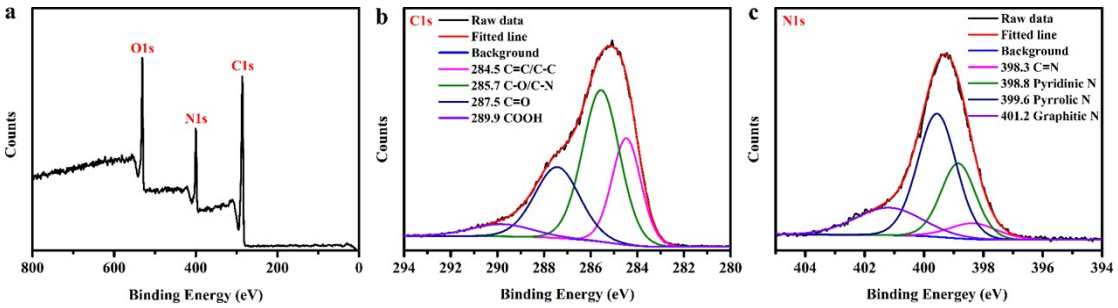

Fig. S4 (a) XPS spectra of the obtained N-CDs; (b-c) high-resolution C 1s and N 1s XPS spectra of N-CDs, respectively.

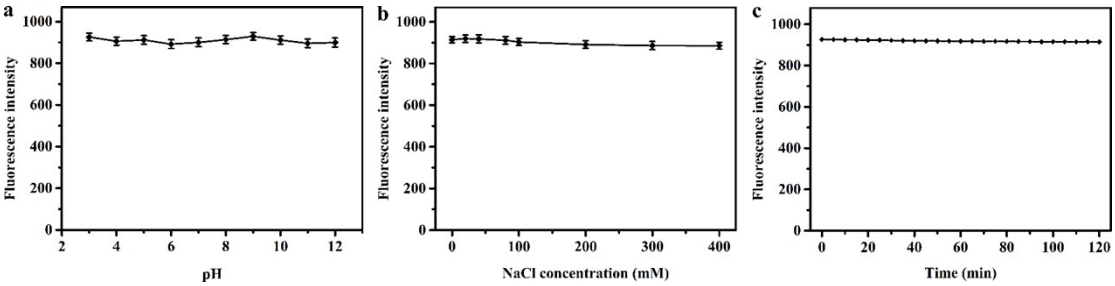

Fig. S5 (a) The fluorescence intensity of N, S-codoped CDs at different pH values; (b) Effect of NaCl concentration on the fluorescence intensity of N, S-codoped CDs; (c) Photostability of N, S-codoped CDs irradiated by xenon lamp for different amounts of time.

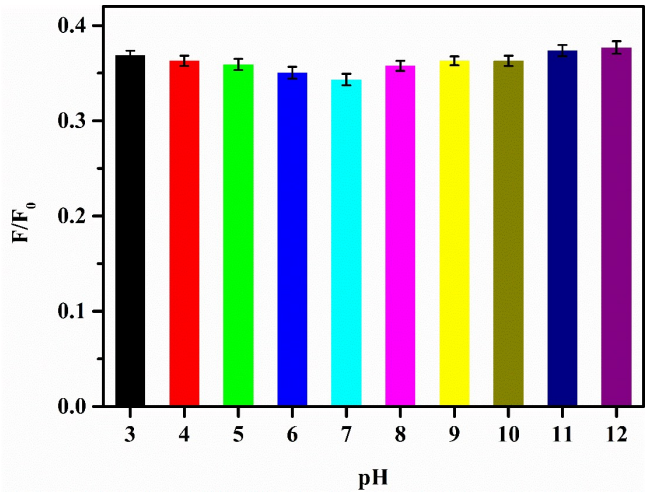

Fig. S6 Fluorescence intensity ratios (F/F_0) of N, S-codoped CDs before and after the addition of Fe^{3+} ions (300 μM) in the presence of 2.5 mM EDTA at different pH values.

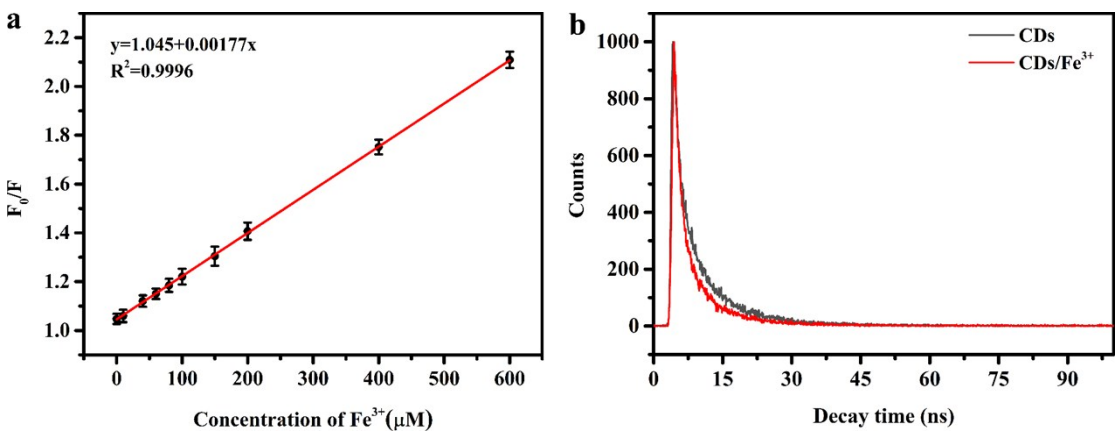

Fig. S7 (a) The linear regression curve of F_0/F versus Fe^{3+} concentration ranging from 0.2 to 600 μM; (b) Fluorescence decay curve of N, S-codoped CDs in the absence and presence of Fe^{3+} ions with excitation at 370 nm.

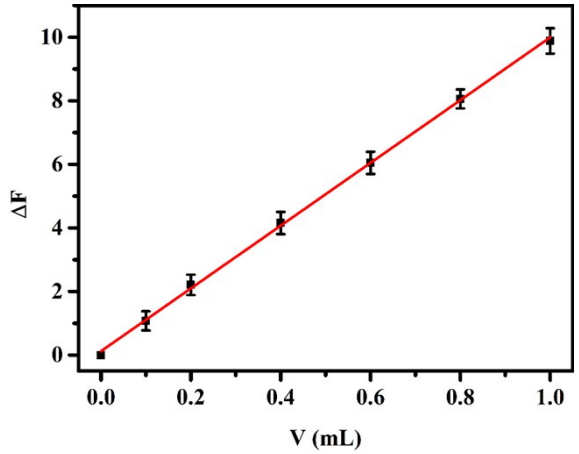

Fig. S8 The relationship between fluorescent quenching values (ΔF) of N, S-codoped CDs and the volume of deproteinized human serum added.

Table S1. Comparison of the QYs and production yields of N, S-codoped CDs synthesized from different aliphatic amine precursors under their respective optimum reaction conditions.

Sample	Optimum reaction conditions			QY (%)	Yield (%)	Price[a] (1 L/USD)
EDA-derived CD	EDA, 4.0 mL	H_2O, 0.5 mL	$Na_2S_2O_8$, 1.0 g	31.5	8.2	57.30
DETA-derived CD	DETA, 2.5 mL	H_2O, 2.0 mL	$Na_2S_2O_8$, 1.0 g	27.8	16.0	69.90
TETA-derived CD	TETA, 1.0 mL	H_2O, 3.5 mL	$Na_2S_2O_8$, 1.0 g	23.7	34.6	95.60
TEPA-derived CD	TEPA, 0.5 mL	H_2O, 4.0 mL	$Na_2S_2O_8$, 1.0 g	26.4	58.0	77.30
PEHA-derived CD	PEHA, 0.3 mL	H_2O, 4.2 mL	$Na_2S_2O_8$, 1.0 g	22.5	56.5	96.20

a. The costs per liter of various aliphatic amine precursors (for synthesis) as quoted by Sigma-Aldrich.

Table S2. The relative atomic ratios of C species for N, S-codoped CDs and N-CDs samples based on XPS analysis.

Sample	C=C/C-C (at%)	C-O/C-N(at%)	C=O/COOH (at%)
N, S-codoped CDs	27.53	57.31	15.16
N-CDs	24.48	44.39	31.14

Table S3. The relative atomic ratios of N species for N, S-codoped CDs and N-CDs samples based on XPS analysis.

Sample	C=N (at%)	Pyridinic N (at%)	Pyrrolic N (at%)	Graphitic N (at%)
N, S-codoped CDs	13.69	9.53	16.58	60.20
N-CDs	7.57	26.17	47.78	18.48

Table S4. Comparison of the present method with other fluorescent nanoprobes about the detection of Fe^{3+}.

Fluorescent nanoprobes types	Sensing system	Detection limit (μM)	Linear range (μM)	Reference
Fluorescent dyes	Azaindole derivative	0.56	2-25	[53]
	Pyrazoline derivative	1.4	0-200	[54]
Fluorescent organic nanoparticles	PDA-derived FONs	0.15	0.5-20	[42]
	PEP-derived FONs	0.67	2-200	[55]
Carbon dots	ATP-derived CDs	0.33	1-150	[52]
	Citric acid-derived CDs	17.9	not given	[56]
	Dopamine-derived CDs	0.32	0-20	[57]
	ASA-derived CDs	0.52	1-250	[58]
	Citric acid-derived CDs	2.0	0-250	[59]
	Rice residue-derived CDs	0.75	3.32-32.26	[60]
	TEPA-derived CDs	0.10	0.2-600	This work

Table S5. Analytical results for the detection of Fe^{3+} ions in environmental water samples by using the as-prepared N, S-codoped CDs.

Samples	Spiked (μM)	Found (μM)	RSD (%, n=6)	Recovery (%)
River water	5.0	4.97	5.16	94.1
	15.0	15.63	6.36	104.2
	25.0	26.27	5.74	105.1
Tap water	5.0	4.97	2.93	99.5
	15.0	15.35	1.43	102.4
	25.0	24.43	6.06	97.7
Lake water	5.0	4.94	6.51	98.9
	15.0	16.19	1.42	107.9
	25.0	24.21	0.60	96.9